Ticagrelor alleviates high-carbohydrate intake induced altered electrical activity of ventricular cardiomyocytes by regulating sarcoplasmic reticulum–mitochondria miscommunication

Yusuf Olgar[1] · Aysegul Durak[1] · Sinan Degirmenci[1] · Erkan Tuncay[1] · Deniz Billur[2] · Semir Ozdemir[3] · Belma Turan[1,4]

Abstract

Metabolic syndrome (MetS) is associated with additional cardiovascular risk in mammalians while there are relationships between hyperglycemia-associated cardiovascular dysfunction and increased platelet P2Y12 receptor activation. Although P2Y12 receptor antagonist ticagrelor (Tica) plays roles in reduction of cardiovascular events, its beneficial mechanism remains poorly understood. Therefore, we aimed to clarify whether Tica can exert a direct protective effect in ventricular cardiomyocytes from high-carbohydrate diet-induced MetS rats, at least, through affecting sarcoplasmic reticulum (SR)–mitochondria (Mit) miscommunication. Tica treatment of MetS rats (150 mg/kg/day for 15 days) significantly reversed the altered parameters of action potentials by reversing sarcolemmal ionic currents carried by voltage-dependent Na^+ and K^+ channels, and Na^+/Ca^{2+}-exchanger in the cells, expressed P2Y12 receptors. The increased basal-cytosolic Ca^{2+} level and depressed SR Ca^{2+} load were also reversed in Tica-treated cells, at most, though recoveries in the phosphorylation levels of ryanodine receptors and phospholamban. Moreover, there were marked recoveries in Mit structure and function (including increases in both autophagosomes and fragmentations) together with recoveries in Mit proteins and the factors associated with Ca^{2+} transfer between SR–Mit. There were further significant recoveries in markers of both ER stress and oxidative stress. Taken into consideration the Tica-induced prevention of ER stress and mitochondrial dysfunction, our data provided an important document on the pleiotropic effects of Tica in the electrical activity of the cardiomyocytes from MetS rats. This protective effect seems through recoveries in SR–Mit miscommunication besides modulation of different sarcolemmal ion-channel activities, independent of P2Y12 receptor antagonism.

Keywords Metabolic syndrome · Arrhythmia · Insulin resistance · Electrical activity · Heart dysfunction · Mitochondria · Sarcoplasmic reticulum · Oxidative stress

Introduction

Metabolic syndrome (MetS) can be defined by the response to high-carbohydrate intake and represents a constellation of markers that indicates a predisposition to diabetes and cardiovascular disease besides other pathologic states [1, 2]. The pathophysiology of MetS includes very complex physiological events, at most, due to multiple interconnected mechanisms, including disturbances in insulin signaling [3, 4]. Similar to others, previously, we have demonstrated high-carbohydrate diet-induced MetS, which is characterized by marked insulin resistance, and associated cardiac dysfunction in rats, including an electrophysiological remodeling in left ventricular cardiomyocytes via alterations in cellular Ca^{2+}-homeostasis and prolongation in action potential (AP) duration [4, 5]. Furthermore, there were marked alterations

✉ Semir Ozdemir
  osemir@akdeniz.edu.tr

✉ Belma Turan
  belma.turan@medicine.ankara.edu.tr;
  belma.turan@lokmanhekim.edu.tr

1 Faculty of Medicine, Department of Biophysics, Ankara University, Ankara, Turkey

2 Faculty of Medicine, Department of Histology and Embryology, Ankara University, Ankara, Turkey

3 Faculty of Medicine, Department of Biophysics, Akdeniz University, Antalya, Turkey

4 Faculty of Medicine, Department of Biophysics, Lokman Hekim University, Ankara, Turkey

in the sarcoplasmic reticulum (SR) and mitochondria functions, parallel to increased oxidative and nitrosative stress markers as well as morphological changes in these organelles from those cells. Recently, it has been shown that depolarization in mitochondrial membrane potential increases in reactive oxygen species (ROS) and intracellular resting level of Ca^{2+}, and decreases in ATP level as well as the increased number of autophagosomes and degeneration of mitochondrion in insulin resistance-mimicked ventricular myocytes [6]. It is now well accepted that there is a close link between insulin resistance and redox stress within the cardiomyocytes, which, in turn, affects whole heart function. Interestingly, a P2Y12 receptor antagonist, ticagrelor (Tica) treatment of these cells provided important protection against insulin resistance changes, particularly developed in mitochondria.

The P2Y12 receptors are the predominant receptors involved in the ADP-stimulated activation of the glycoprotein IIb/IIIa receptor [7]. Although P2Y12 receptors have been seen as platelet-specific, many cells express P2Y12 receptors including endothelial cells [8], vascular smooth muscle cells [9] and neurons [10]. Of note, similar to others [11], we recently have shown that P2Y12 receptors are expressed comparatively less amount in heart tissue [6]. However, the roles of these non-platelet P2Y12 receptors are poorly explored, but there are emerging data in the field of cardiac dysfunction independent of hyperactivity of platelets under pathological conditions, including diabetes [12]. However, the clinical relevance of non-platelet P2Y12 receptors and their inhibition, including cardiomyocyte P2Y12, is not exactly known yet.

Particularly, recent clinical studies highlighted the important role of antiplatelet therapy with new generation drugs in diabetics and other patients with heart dysfunction, to reduce the risk of mortality. Among them, a new generation P2Y12 inhibitor, Tica, is more efficacious in protecting organs against new ischemic events and mortality in T2DM and heart failure following acute myocardial infarction [13–16]. Nevertheless, some clinical and experimental results demonstrated Tica treatment benefits are beyond its P2Y12 inhibitor effect such as antibacterial, anti-inflammatory, and antioxidative action, at least partially, attributed to its off-target effects [17–21].

Metabolic disorders in mammalian cells can lead to SR-to-mitochondria miscommunication, while alterations in the interaction of mitochondria with the SR can underline, in part, a dishomeostasis in intracellular Ca^{2+} signaling [22, 23]. Furthermore, there are also relations between autophagy and the controlled level of SR–mitochondria coupling [24, 25]. Therefore, in the light of previous reports and our recent data, we propose that the clinical benefit as a P2Y12 receptor antagonism cannot be limited to platelet inhibition and the prevention of arterial thrombus formation in patients with

metabolic disorders. Potential additional effects should be involved, in particular cardioprotective effects. Supporting this hypothesis, we recently have shown that Tica pretreatment of in vitro insulin resistance developed cardiomyocytes could prevent mitochondrial dysfunction by alleviating the accumulated autophagosomes-dependent apoptosis and ER stress [26]. Furthermore, Tica pretreatment prevented the depletion of ATP and the increased level of oxidative stress. Recent studies have also strongly pointed out the contribution of Tica-associated P2Y12 inhibition beyond thrombosis during various clinical inflammatory diseases, acute lung injury, asthma, atherosclerosis, and cancer. [17, 18, 27–29]. Correspondingly, taken into consideration the relation between increased oxidative stress and mitochondria dysfunction and thereby their roles in cardiovascular disorders (particularly alterations in SR–mitochondria axis) under pathological condition [30], we hypothesize a possible Tica-associated benefit on SR–mitochondria miscommunication in left ventricular cardiomyocytes from high-carbohydrate diet-induced insulin-resistant MetS rats, beyond its platelet P2Y12 receptor antagonism.

Materials and methods

Animals and experimental design

Male Wistar rats (8-week-old) were used and metabolic syndrome (MetS) was induced as described, previously [4]. Briefly, the rats fed with a high-carbohydrate diet (by adding 32% sucrose into their drinking water) for 16 weeks, in addition to their standard chow ad libitum. The experimental design is as follows: The control (Con) group was fed with standard chow ad libitum and had also free access to tap water (n = 8 rats). Following the validation of MetS in rats, as described previously [4] and determined the blood parameters and platelet-reactivity as well, MetS rats were divided into two groups: the MetS group (n = 10 rats) and Tica-treated MetS group (Tica; dissolved in tap water and orally administered (by gavaging) as 150 mg/kg/day for 15 days, n = 10 rats) [30, 31]. The rats from either the control group or MetS group were treated with tap water in an identical fashion to the treatment group for 15 days.

All animals were exposed to a 12 h light–dark cycle and were housed in standard rat cages. All applicable international, national, and/or institutional guidelines for the care and use of animals were followed on the care and use of laboratory animals. All experimental protocols were approved by the Institutional Animal Care and Use Committee of the Ankara University with a reference number of 2016–18-165. All animals received humane care under an institutionally approved experimental animal protocol with ethical license in Turkey.

Validation of MetS

Blood glucose levels were assessed by standard glucose test strips (GlucoCheck Analyzer). To monitor oral glucose tolerance test, OGTT, all animals were undertaken a test to measure the blood responses to an intake of concentrated glucose solution (75 g) at 0th, 15th, 30th, 60th, and 120th min. The development of insulin resistance with this diet was determined by HOMA-IR index [4]. Platelet-reactivity was determined by measuring the prothrombin time in a test tube. The rats with MetS have a normal complete blood count and platelet-reactivity. Briefly, the blood was drawn into a test tube containing liquid sodium citrate (3.8%), which acts as an anticoagulant by binding the calcium in a sample. The blood is mixed, then centrifuged (1000 g for 10 min) to separate blood cellular compartments from plasma. A sample of the plasma is extracted from the test tube and mixed with excess of calcium thromboplastin to saturate citrate and allowing forming a time dependent clot again. All experiments were performed at 37 ± 1 °C.

Isolation procedure of cardiomyocytes from the left ventricle of the heart

Freshly cardiomyocyte isolation was performed enzymatically, as described previously [32]. Briefly, following a rapid excise of hearts and cannulation of aortas to the Langendorff perfusion system, they were perfused retrogradely at 37 °C with a Ca^{2+}-free, HEPES-buffered solution for 5–7 min. Then, the perfusion was continued by switching a solution supplemented with 1.0–1.3 mg/mL collagenase (Type A, Worthington) for 30–40 min. Following this procedure, the hearts were removed from the perfusion system and the left ventricle was separated. Then minced ventricle is filtered through nylon mesh. The dispersed cardiomyocytes were then suspended in HEPES-buffer supplemented with 1 mM Ca^{2+} and 0.5% bovine serum albumin (pH at 7.4). Cardiomyocytes were kept at 37 °C during the day (up to 6 h) for electrophysiological examinations.

Measurements of action potentials and ionic currents

All electrophysiological recordings in freshly isolated left ventricular cardiomyocytes were recorded using Axoclamp patch-clamp amplifier (Axopatch 200B amplifier, Axon Instruments, USA) at 21 ± 2 °C. Online recorded data were sampled and digitized at 5 kHz using an analog-to-digital converter and software (Digidata 1200A and pCLAMP 10.0; Axon Instruments, USA).

The amplifier has been used in the current-clamp mode to record AP, as described previously [5]. The resting membrane potential, the maximum amplitude of APs, and AP duration from the repolarization phase at 25, 50, 75, 90% ($APD_{25,50,75,90}$), were calculated from original records (at least 12–16 records/cell).

To determine ionic currents, the amplifier has been used in the voltage-clamp mode as a whole-cell configuration. We first recorded TTX-sensitive voltage-dependent Na^+ channel currents (I_{Na}) as described, previously [5]. During current recordings, cells were superfused with a low Na^+-HEPES solution of the following composition (mmol/L): NaCl 40, N-methyl-D-glucamine 77, CsCl 20, $CaCl_2$ 1.8, $MgCl_2$ 1.8, $CdCl_2$ 0.2, glucose 10, HEPES 10 and pH at 7.4 with HCl. We used a pipette solution contained (in mmol/L) CsCl 120, Mg-ATP 5, HEPES 20, EGTA 5, Na-GTP 0.4, and pH adjusted to 7.2 with CsOH.

L-type Ca^{2+} channel current (I_{CaL}) measurement was performed using the whole-cell patch-clamp technique, as described previously [5]. Briefly, currents were recorded at room temperature (22 ± 2 °C) in the presence of CsCl to inhibit K^+ currents. The TTX-sensitive Na^+ channel currents (I_{Na}) were inhibited after a voltage ramp protocol from a holding potential of –80 mV to a prepulse at –45 mV. Patch pipettes (1.5–2.0 M) were filled with a solution (in mmol/L; 110 Cs-Aspartate, 120 CsCl, 5.0 Mg-ATP 120 L-Aspartate, 10 NaCl, 10 HEPES, 0.4 GTP, 10 HEPES and pH at 7.3). Cells were held at –80 mV and I_{CaL} amplitude was estimated as the difference between peak inward current and the current level at the end of the 300 ms voltage pulse.

Second, we examined the Na^+/Ca^{2+}-exchanger (NCX) current (I_{NCX}) in the isolated cardiomyocytes. Both inward and outward parts of I_{NCX} were recorded with a protocol composed of a descending ramp from + 80 to –120 mV at a holding potential of –40 mV. The recording solution was included (as mM) NaCl 130, TEA-Cl 10, Na-HEPES 11.8, $MgCl_2$ 0.5, $CaCl_2$ 1.8, ryanodine 0.005, nifedipine 0.02, glucose 10 with pH at 7.4. The pipette solution (as mM) was CsCl 65, $CaCl_2$ 10.92, EGTA 20, HEPES 10, Mg-ATP 5, $MgCl_2$ 0.5, TEA-Cl 20 with pH at 7.2. In the presence of chelators we determined 180 nM free Ca^{2+} in the pipette solution.

We also recorded voltage-dependent K^+ channel currents (I_K) as described, previously [5]. Briefly, the bath solution contained (as mM) 137 NaCl, 4 KCl, 1.8 $CaCl_2$, 1 $MgCl_2$, 10 glucose, and 10 HEPES adjusted pH at 7.4. The patch-pipette solution was containing (as mM) 140 KCl, 3 Mg-ATP, 5 EGTA, and 25 HEPES at pH 7.2. The total currents were recorded in the presence of external Cd^{2+} (250 µM) and the holding potential was –80 mV, while I_{Na} was inactivated with a ramp-voltage protocol. Both inward and outward parts of the current were calculated at -120 mV and + 70 mV, respectively. For correct comparison among groups, all types of current recordings were divided by relevant cell capacitances whereby the current densities were calculated and the results were expressed as pA/pF.

Monitoring of diastolic Ca²⁺ leak from ryanodine receptors

To monitor the basal level of intracellular free Ca^{2+}, we used calcium ion-specific fluorescence dye (4-μM Fura-2AM) loaded cardiomyocytes. Following the loading of the cells, the recordings in the fluorescence intensity changes were performed using a ratiometric microspectrofluorometer (PTI Ratiomaster and FELIX software; Photon Technology International, Inc., NJ USA), as described previously [5]. All fluorescence intensity changes were measured at 21 ± 2 °C. The changes in fluorescence intensities are presented as intracellular free Ca^{2+} level changes.

Monitoring of sarcoplasmic reticulum Ca²⁺ load

Following the basal level of cytosolic Ca^{2+} (as intensity changes) in resting cardiomyocytes, the SR load and the state of the SR Ca^{2+}-ATPase (SERCA2) were measured by the determination of SERCA2-mediated Ca^{2+}-reuptake in the same basal level of cytosolic Ca^{2+} measured in the cardiomyocytes, as described earlier, as well [33]. Briefly, after electric field stimulation, Fura-2AM loaded cells were perfused with a solution contained 0 Na^+/0 Ca^{2+}, by replacing NaCl and $CaCl_2$ with equimolar NMDG or 10 mmol/L EGTA, respectively. Following this procedure, the loaded cells were stimulated with a 10 mmol/L caffeine for 1 s to induce full Ca^{2+} release from SR. Then, the level of intracellular free Ca^{2+} was measured in the presence of tetracaine, giving Ca^{2+} leak from ryanodine receptors, RyR2s, and SR Ca^{2+} content.

Histological analysis of isolated cardiomyocytes

Either the heart tissue or isolated left ventricular cardiomyocytes were examined using light and electron microscopy. Briefly, samples were fixed with 0.2 M phosphate buffer containing 2.5% glutaraldehyde and 2% paraformaldehyde mixture solution (pH at 7.3) for 2–4 h at room temperature. Following the dehydration of samples with an ethanol series, the specimens were embedded in Araldite 6005 and cut with a Leica Ultracut R (Leica, Solms, Germany) ultramicrotome. Ultra-thin sections, stained with uranyl acetate and lead citrate, were examined using an LEO 906 E TEM (80 kV, Oberkochen, Germany) and photographed with a CCD and Image SP (Germany) digital imaging system.

Mitochondrial membrane potential and ROS monitorization by confocal microscopy

The mitochondrial membrane potential ($\Delta\Psi$m) of freshly isolated cardiomyocytes was measured using a potential sensitive fluorescence dye JC-1, as described previously [33].

Briefly, the cells were loaded with 5-μM JC-1 for 30 min and then imaged with a confocal fluorescence microscope (Leica TCS SP5). The probes were excited at 488 nm and the red fluorescence image was detected at both 535 nm and 585 nm and carbonylcyanide 4-(trifluoromethoxy)phenylhydrazone, FCCP (5-μM acute application) were used for calibration.

The cellular ROS production in freshly isolated cardiomyocytes was measured as described elsewhere [33]. The cells were loaded with a ROS indicator chloromethyl-2′,7′-dichlorodihydrofluorescein diacetate, DCFDA (5-μM for 1-h incubation). DCDFA was excited at 488-nm and emission collected at 560-nm wavelengths with a laser scanning confocal microscope (LEICA TCS SP5). To obtain maximal fluorescence intensity associated with ROS production, the cells were exposed to H_2O_2 (100-μM), acutely. The fluorescence changes, as peak values, ($\Delta F/F0$, where $\Delta F = F - F_0$ and F_0 represents basal fluorescence level while F is the local maximum elevation of fluorescence intensity) is calculated from confocal images. All fluorescence changes are given as percentage changes in the manuscript.

Western-blot analysis

The cells were prepared for Western-blot analysis, as described by elsewhere [11]. Equal amount of protein preparations were run on SDS–polyacrylamide gels and blotted with a primary antibody against P2Y12 (Abcam, ab184411, 1:3000), phospho-casein kinase 2 (Invitrogen, PA5-37,540, 1:600), casein kinase 2 (Santa Cruz, sc-12738, 1:200), pRyR2²⁸¹⁴ (Badrilla, A010-31, 1:1000), RyR2 (Santa Cruz, sc-8170, 1:1000), SERCA (Santa Cruz, sc-376,235, 1:500), pPLB (pPLBᵀʰʳ¹⁷; sc-17,024, 1:10 000), PLB (PLB; sc30142, 1:1000), Mnf-1 (sc-166,644, 1:1000), Mnf-2 (sc-100,560, 1:1000), PML (sc-966, 1:1000), pNOS3 (Ser¹¹⁷⁷; Santa Cruz, sc-12,972, 1:250), NOS3 (Santa Cruz, sc-654, 1:250), GRP78 (Santa Cruz, Sc13968; 1:200), calregulin (Santa Cruz, sc-11398 1:200), β-actin (Santa Cruz, sc-47778, 1:5000) and GAPDH (Cell Signaling, D16H11, 1:5000) to detect their protein levels.

Determination of oxidative/antioxidative status

Total Oxidant Status (TOS) and Total Antioxidant Status (TAS) levels were measured in tissue homogenates using commercially available kits as described elsewhere [6]. TAS levels in homogenates was measured using a commercially available kit (RL0024, Rel Assay Diagnostics, Turkey), as described previously [31]. This method is briefly based on the bleaching of a characteristic color of a more stable ABTS (2,2 = − azino-bis (3-ethylbenzothiazoline-6-sulfonic acid)) radical cation by antioxidants. The results are expressed as mmol Trolox equivalent/L. TOS level in tissue homogenates was measured using

commercially available kits (RL0024, Rel Assay Diagnostics, Turkey). Briefly, the oxidation reaction is enhanced by glycerol molecules abundantly present in the reaction medium. The ferric ion produced a colored complex with xylenol orange in an acidic medium. The color intensity, measured spectrophotometrically, is related to the total amount of oxidant molecules present in the sample. The assay is calibrated with H_2O_2, and the results are expressed in mol/L H_2O_2 equivalent/L.

Reagents and statistical analysis of data

Chemicals were obtained from Sigma-Aldrich (St. Louis, MO) unless otherwise stated. Data were presented as mean $\pm$ SEM with GraphPad Prism 6.0 (GraphPad Software, Inc, La Jolla, CA). Comparisons between quantitative variables were assessed using either the Student's t-test or one-way ANOVA at a 0.05 level of significance.

Results

No beneficial effects of Tica treatment on the metabolic indexes of MetS rats

We, first, confirmed the development of the MetS in rats, fed with a high-carbohydrate diet, by determination of body weight, blood glucose level, and OGTT values. As can be seen in Fig. 1 (A-to-D), Tica treatment of those rats did not induce any significant beneficial effects ($p > 0.05$) on high body weight and high fasting blood glucose levels of MetS rats (A and B). Furthermore, we determined the peak blood glucose levels measured at 15th, 30th, 60th, and 120th min during the OGTT monitoring in the Tica-treated MetS group compared to that of either MetS or control group, and then, we calculated the areas under OGTT curves. The calculated areas for these three groups were similar and there were no significant differences between them ($p > 0.05$), as well (C). Interestingly, cardiomyocyte dimension (given as
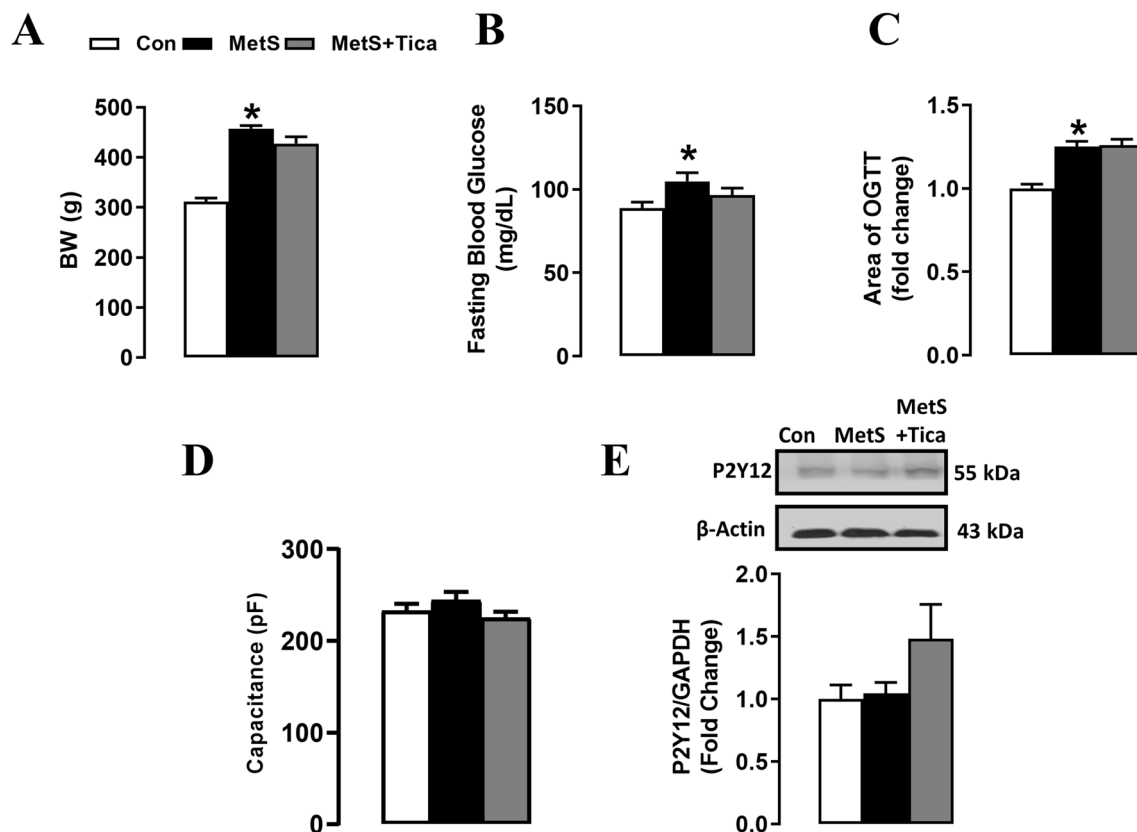

Fig. 1 General parameters of experimental animals. Bodyweight (BW) (**A**), fasting blood glucose (**B**), the area under curves of the oral glucose tolerance test (OGTT) determined between 0–120 min (**C**), the cell capacitance as a measure of cell size (**D**) determined in ticagrelor (Tica)-treated and untreated metabolic syndrome (MetS) rats compared to those of controls (Con). (**E**) The protein expression level of P2Y12 was measured in the isolated ventricular cardiomyocytes. All data were presented as mean $\pm$ SEM. The total number of rats in each group; Tica-treated MetS rats (Tica + MetS: 150 mg/kg/day for 15 days), metabolic syndrome rats (MetS: 32% high sucrose feeding for 16 weeks), and age-matched normal rats, control rats. The number of rats per group: $n_{Tica} = 10$, $n_{MetS} = 8$, and $n_{Con} = 8$. Significance level, $^*p < 0.05$ vs. Con group, $^*p < 0.05$ vs. MetS group

capacitance; pF) did not differ among the groups, as well (D).

The MetS group compared to that of control group has a complete blood count (data not given). The platelet activity of MetS rats was determined by measuring the time dependent clot formation referred prothrombin time. The average (mean $\pm$ SEM) prothrombin time was (40.3 ± 4.0) s in the MetS group while that value was (35.3 ± 2.3 s) in the control group. The differences between these two groups were not statistically different ($p > 0.05$).

The protein expression level of P2Y12 receptors in both normal and MetS rats

Although the protein expression level of P2Y12 receptors is low in the mammalian heart [11], we, previously, determined its mRNA level in the H9c2 cell-line [6]. Here, we also performed Western blotting in the isolated ventricular cardiomyocytes and determined a considerably detectable protein expression levels among the experimental groups. As can be seen in Fig. 1E, there is a measurable level of P2Y12 receptor protein level in the control group cardiomyocytes and that level was not different in either the MetS or Tica-treated MetS group ($p > 0.05$).

Ticagrelor treatment of MetS rats prevented the alterations in the action potential configuration of the isolated cardiomyocytes

The original AP recordings in isolated cardiomyocytes from the left ventricle of rat heart in MetS, ticagrelor-treated MetS, and age-matched controls are given in Fig. 2A, as superimposed with horizontally shifted traces for sake of clarity. Similar to our previous studies [5], there was a significantly increased amplitude of APs with no change in resting membrane potentials of the
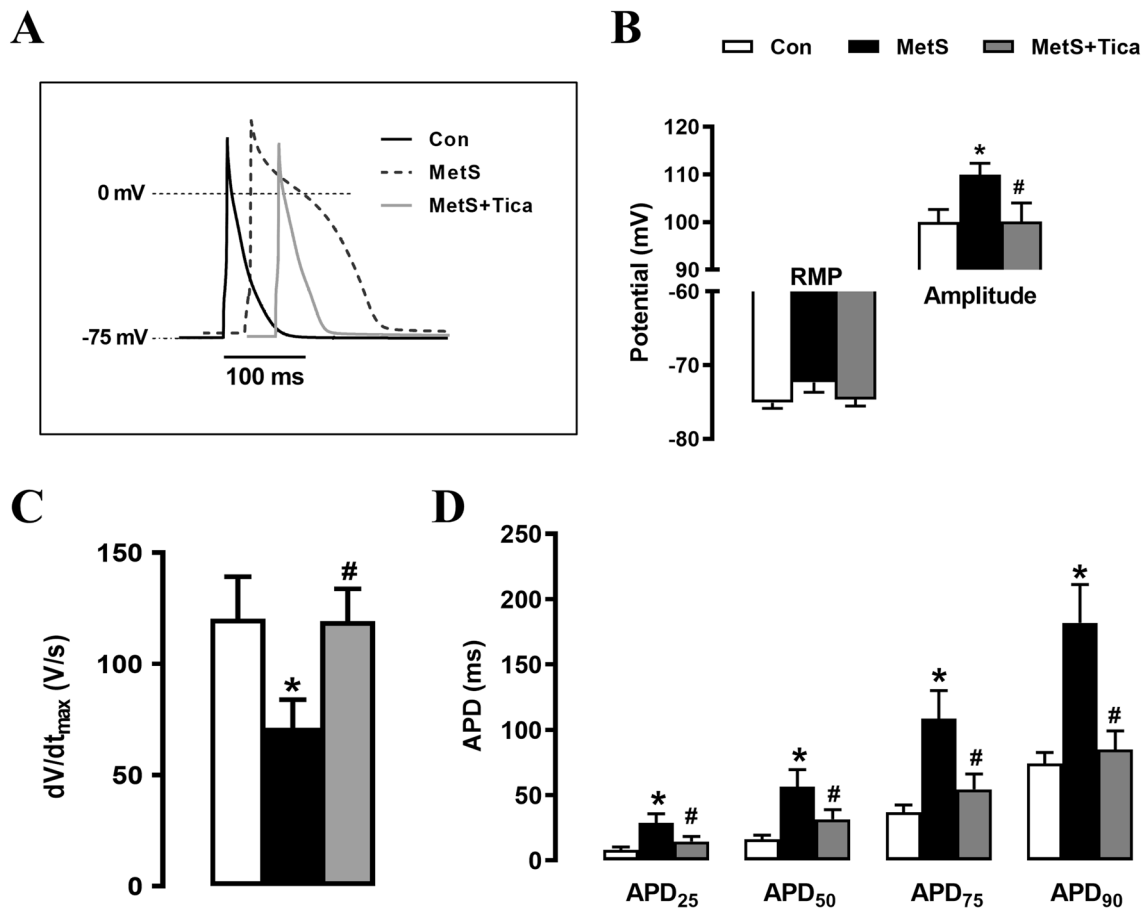

Fig. 2 Effect of ticagrelor treatment on action potential parameters in left ventricular cardiomyocytes from MetS rats. (**A**) Representative action potential (AP) traces of cardiomyocytes from Tica-treated MetS rats comparison to untreated MetS rats or normal fed age-matched control (Con) rats. (**B**) The resting membrane potentials of the cells (left) and the amplitude of AP (right). (**C**) The derivatives of the depolarization phases of APs are calculated for each group. (**D**) AP duration measured at 25, 50, 75, 90% of repolarizations (APD_{25}, APD_{50}, APD_{75}, APD_{90}) given for all groups. The total number of cells, used for each protocol, is 12–18 cells isolated from 4–5 rats. Significance level at $^*p < 0.05$ vs. Con group and $^\#p < 0.05$ vs. MetS group

cardiomyocytes from the MetS group compared to those of controls ($p > 0.05$) (Fig. 2B, left). The upstroke amplitudes of APs in MetS group were significantly higher than those of controls ($p < 0.05$), while Tica treatment of MetS rats significantly prevented that increase ($p < 0.05$) (Fig. 2B, right).

To better understand whether there is a slowdown in the time to overshoot potential, we calculated the rate of change of depolarization with time by measuring the maximum value of depolarization slope of the APs (dV_{max}/dt). As can be seen in Fig. 2C, MetS induced a marked slowdown (about 40% *vs.* control) in the depolarization rate of the APs ($p < 0.05$) while it was fully recovered with Tica treatment ($p < 0.05$).

Similar to our previous studies [5, 34], the duration of APs measured at 25, 50, 75, and 90% repolarization of APs (APD25, APD50, AP75, and APD90) were prolonged significantly in the MetS group ($p < 0.05$), while they were fully reserved by ticagrelor treatment of MetS rats ($p < 0.05$) (Fig. 2D).

The effects of ticagrelor treatment on sarcolemmal ionic currents in MetS rat cardiomyocytes

We determined the ionic current contributes to the depolarizing phase of the APs. For this aim, first, the current–voltage relation (I–V) of voltage-gated Na^+ channel currents (I_{Na}), the maximum amplitude of I_{Na}, and their time courses are calculated for these three groups. As can be seen in Fig. 3A, the current–voltage (I–V) characteristic of these channels measured in MetS group was significantly different from that of the control group ($p < 0.05$) while the (I–V) curve of the Tica-treated MetS group was fitting to that of the control group (right). However, there were no significant differences between the voltage-dependency of these three groups ($p > 0.05$). The original current recordings for these three groups are given in the left of the Fig. 3A. The maximum amplitude of I_{Na}, measured at -40 mV was significantly high in the MetS group than the control group ($p < 0.05$) while Tica treatment provided a full restoration ($p < 0.05$) (Fig. 3B).
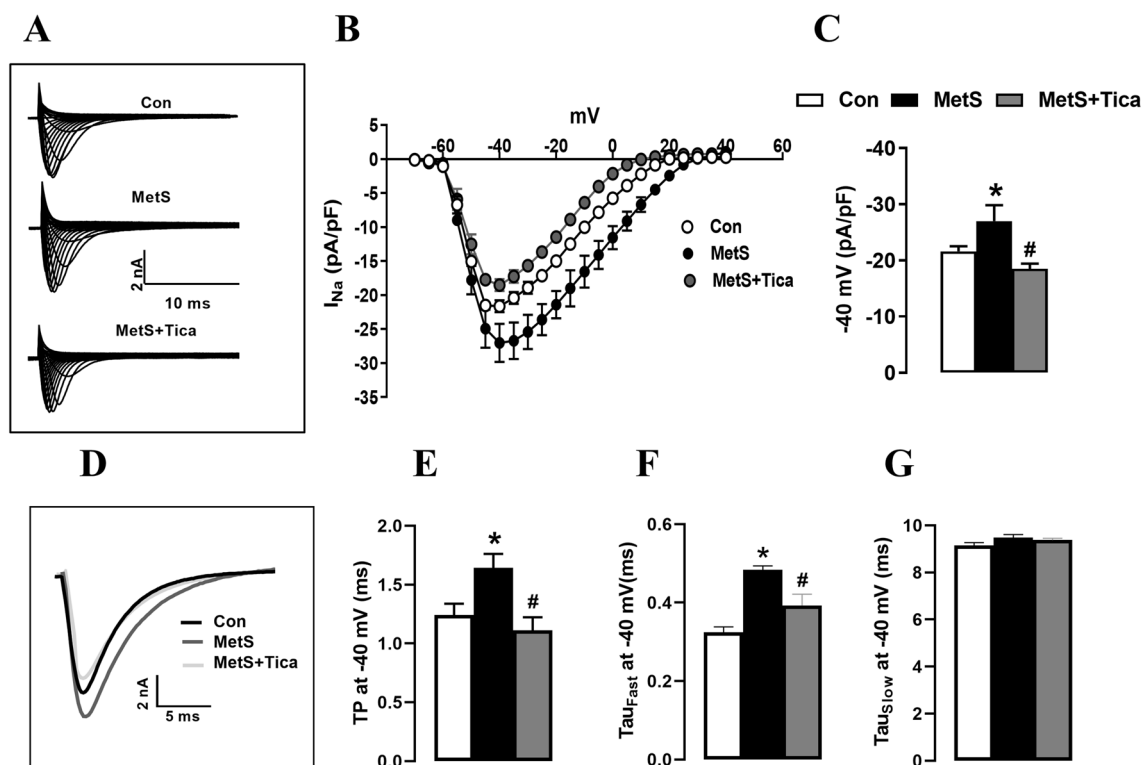

Fig. 3 Effects of ticagrelor treatment of MetS rats on voltage-dependent Na^+ channel currents in left ventricular cardiomyocytes. (**A**) The representative voltage-dependent Na^+ channel currents (I_{Na}) (left) and (**B**) the current–voltage relationships (I–V characteristics) of those voltage-dependent Na^+ channels (right). (**C**) The calculated maximum I_{Na} values at -40 mV are given. (**D**) The original current traces to calculated the time to peak activation and inactivation of I_{Na} at -40 mV. (**E**) Time to peak of activation of I_{Na} at -40 mV among the groups. Inactivation of the currents at -40 mV were fitted the exponential equation ($y = A_i te^{-/\tau i} + C$ equation to obtain (**F**) Tau_{Fast} and (**G**) Tau_{Slow}, respectively. The bar graphs are representing mean ($\pm$ SEM) values. The number of cells used for every protocol for every group, $n_{cell} = 12$–15, number of rats for every group; $n_{rat} = 4$–5. Significance level at $^*p < 0.05$ *vs.* Con group and $^\#p < 0.05$ *vs.* MetS group

Since there was a slowdown in the depolarization phase of APs of the MetS group, although APs amplitudes are significantly high (given in Fig. 2C), we analyzed the time to peak of the activation as well as inactivation of I_{Na} (tau constants), as both fast and slow components. As can be seen in Fig. 3D–G, there were significant slowdowns in the MetS group ($p < 0.05$), while they were recovered with Tica treatment ($p < 0.05$) (left and right, respectively).

In another set of experiments, we examined the ionic currents that can mainly contribute to repolarization of APs. We monitored the voltage-dependent L-type Ca^{2+} channel currents (I_{CaL}) and voltage-dependent K^+ channel currents (I_K). As can be seen in Fig. 4A, the current–voltage (I–V) characteristics of voltage-dependent L-type Ca^{2+} channels, as well as the time courses (data not shown) measured in the MetS group, are no different from those of controls ($p > 0.05$), while Tica treatment could not affect those parameters of that current, as well ($p > 0.05$).

Furthermore, we also examined the Na^+/Ca^{2+}-exchanger currents (I_{NCX}) in both forward and reversed directions (I_{NCXin} and I_{NCXout}, respectively) in the cardiomyocytes from MetS rats compared to those of controls. In reverse but not forward direction, the maximum amplitude of I_{NCX} was significantly higher in the MetS group compared to the control group ($p < 0.05$) (Fig. 4B). Tica treatment of MetS rats provided a full recovery in the maximum amplitude of that current measured in a reversed direction ($p < 0.05$) (inset).

We, also, examined the I_K values in the cardiomyocytes from Tica-treated MetS rats, measured between -120 mV and $+70$ mV voltage ranges (Fig. 4C). These currents (the maximum amplitude of that current measured at $+70$ mV) were significantly depressed in the MetS group compared to those of the controls ($p < 0.05$), while they were fully normalized in the Tica-treated MetS group (Fig. 4D). The original current recordings for these three groups are given in the left part of Fig. 4C.
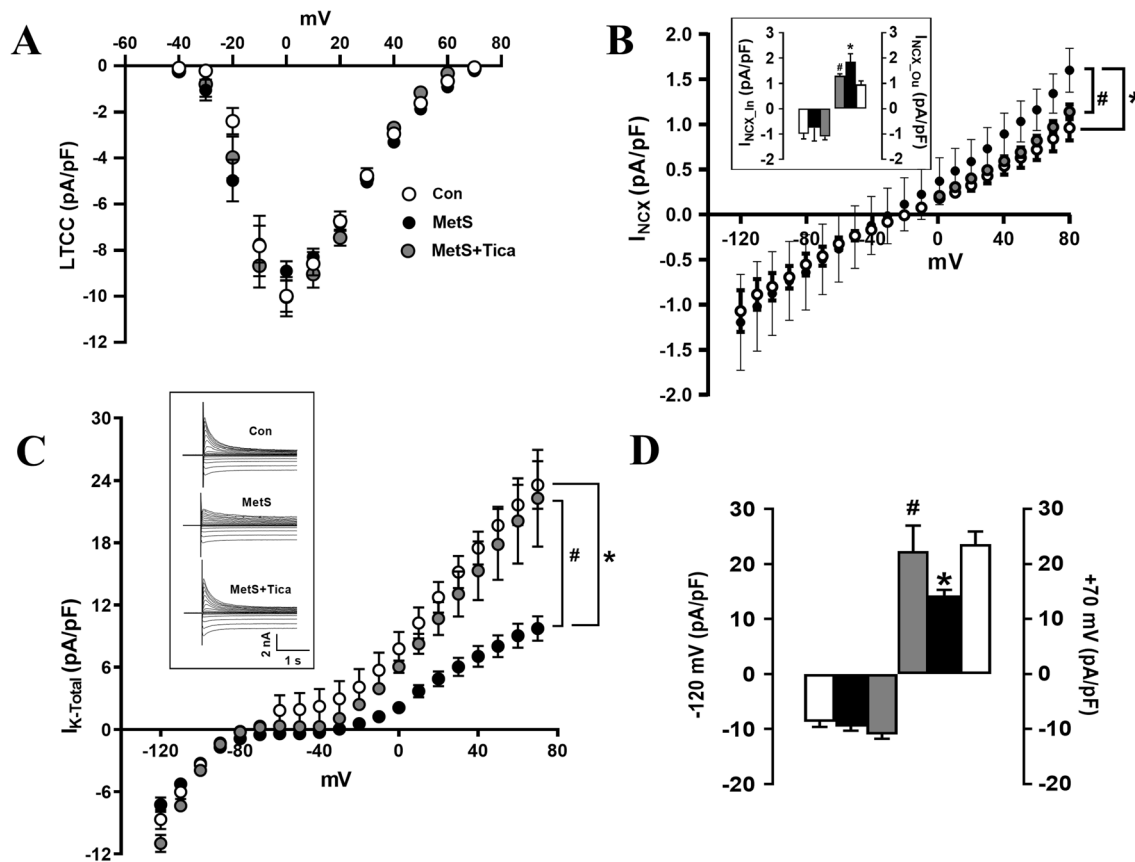

Fig. 4 Effects of ticagrelor treatment on voltage-dependent L-type Ca^{2+} channel and K^+ channel currents and Na^+/Ca^{2+}-exchanger currents in left ventricular cardiomyocytes. (**A**) The (I–V) characteristics of voltage-dependent L-type Ca^{2+} channel currents (I_{CaL}) for the Tica-treated and untreated MetS group compared to that of the control group. (**B**) The I–V characteristics of I_{NCX} in both directions (forward; I_{NCXin} and reversed; I_{NCXout}) and their maximum values measured at -120 mV and $+80$ mV (inset). (**C**) The original repre- sentative voltage-dependent K^+ channel currents (I_K) and their (I–V) characteristics given in inset. (**D**) Calculated maximum I_K measured at -120 mV and $+70$ mV are given as bar graphs. The bar graphs are representing mean ($\pm$ SEM) values. The number of cells used for every protocol for every group, $n_{cell} = 12$–15, number of rats for every group; $n_{rat} = 4$–5. Significance level at $^*p < 0.05$ *vs.* Con group and $^{\#}p < 0.05$ *vs.* MetS group

Ticagrelor treatment of MetS rats induced important benefits on the function of sarcoplasmic reticulum of left ventricular cardiomyocytes from MetS rats

In these set of experiments, to demonstrate the effect of Tica treatment in MetS rats on the basal level of intracellular free Ca^{2+}, we used Fura-2AM loaded freshly isolated left ventricular cardiomyocytes and determined fluorescence intensity changes related to the basal level of intracellular free Ca^{2+}. Therefore, all data are presented as fluorescence intensity changes (as $\Delta F_{340/380}$) in the loaded cells. As shown in Fig. 5A, the $\Delta F_{340/380}$ was significantly higher in the MetS group than the control group ($p < 0.05$), while it was markedly recovered with the Tica treatment.

Second, we aimed to assess the status of diastolic Ca^{2+} levels in cardiomyocytes from the Tica-treated MetS group compared to those of the untreated MetS group. For this aim, we examined SR Ca^{2+} leak with a protocol given in Fig. 5B (right; original recordings with experimental protocols). The SR Ca^{2+} leak (as $\Delta F_{340/380}$) were measured during tetracaine application (1-mM) followed with 10-mM caffeine application. The fluorescence intensity of SR Ca^{2+} leak was about twofold higher in the cardiomyocytes from MetS rats than those of controls, while it was similar to the control value in the Tica-treated MetS rat cardiomyocytes (Fig. 5C, left). Furthermore, we determined the Ca^{2+} released from SR during the caffeine (10-mM) application (as $\Delta F_{340/380}$). As can be seen in Fig. 5C (right), the SR Ca^{2+} content was 50% less in MetS rat cardiomyocytes compared to that of control,
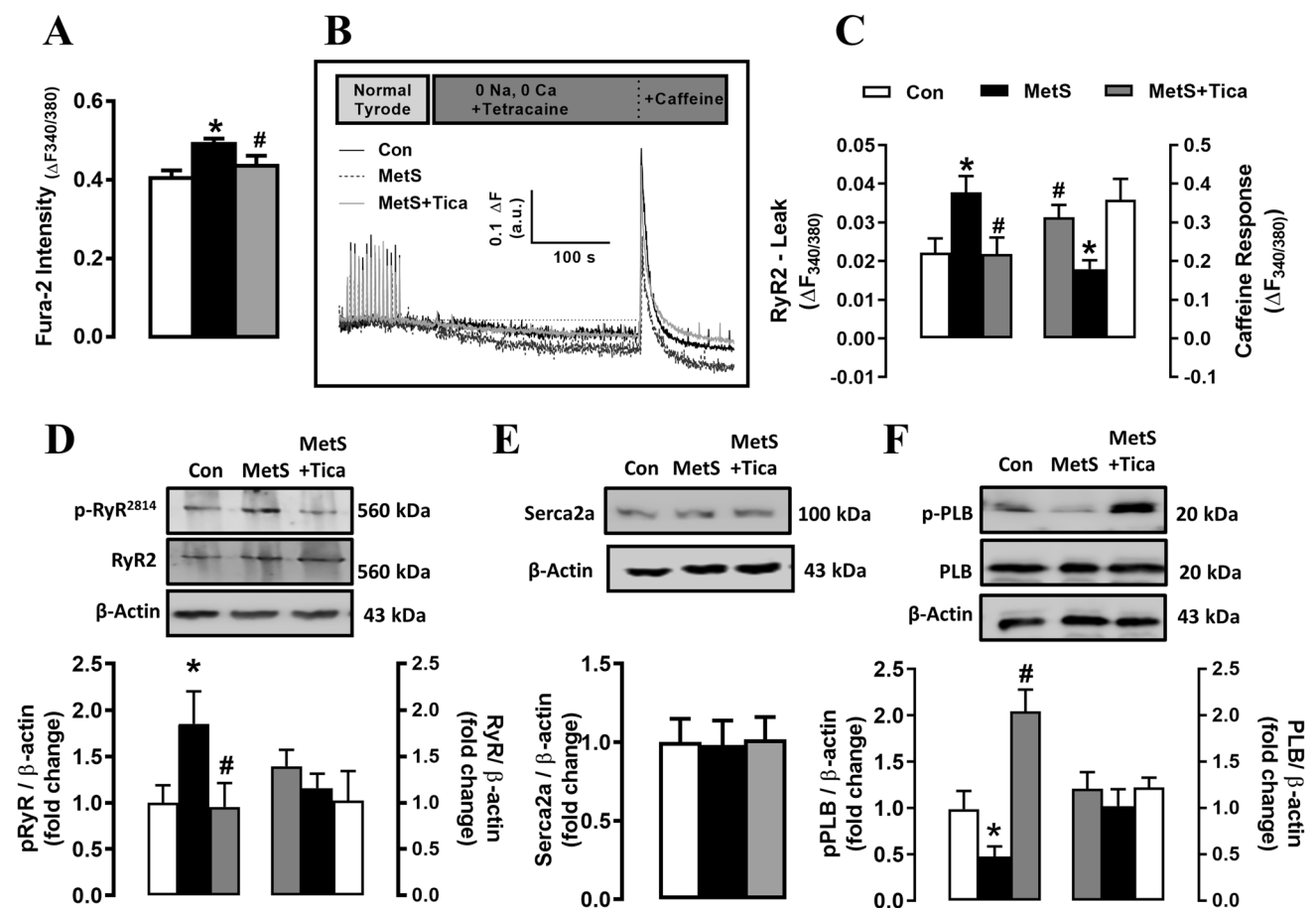

Fig. 5 Ticagrelor treatment of MetS rats provided benefits on the alterations in tetracaine-sensible cytosolic Ca^{2+} stores though affecting Ca^{2+} leakage from SR as well as SR Ca^{2+}-pump activity in left ventricular cardiomyocytes. (**A**) The fluorescence intensity changes (as $\Delta F_{340/380}$ with arbitrary unit), corresponding to the basal levels of cytoplasmic free Ca^{2+}, detected in the cardiomyocytes loaded with Ca^{2+}-sensitive Fura-2AM (4-μM). (**B**) The representative diastolic SR Ca^{2+} release related channels, ryanodine receptors, RyR2, leaks in the presence of tetracaine (1-mM), and caffeine (10-mM) application in the Fura-2AM (4-μM) loaded ventricular cardiomyocytes. (**C**) The mean values of RyR2 leak (left) and caffeine responses (right) were determined as fluorescence intensity changes in those cardiomyocytes. (**D**) The phosphorylation (left) and protein expression (right) levels of RyR2. (**E**) The protein expression levels of SR Ca^2-pump ATPase (SERCA2a). (**F**) The phosphorylation (left) and protein expression (right) levels of phospholamban (PLB). The bars are representing the mean ($\pm$ SEM), the number of hearts is 4–5, and the number of cells is 15–20 for each measurement. *$p < 0.05$ *vs.* Con group and #$p < 0.05$ *vs.* MetS group

while the Tica treatment reversed that decrease, significantly ($p < 0.05$).

To test further whether the beneficial effect of the ticagrelor treatment on the alterations in Ca^{2+} release pattern such as Ca^{2+} leakage from SR is through recovery in the leaky-cardiac RyR2, we determined the protein expression levels of both phospho-RyR2 and total RyR2 in the ventricular cardiomyocytes (Fig. 5D). The total protein level of RyR2 in the MetS group was not significantly different from that of the control group ($p > 0.05$) (right), while the hyperphosphorylated RyR2 (phospho-RyR2) was found to be restored significantly in Tica-treated MetS rat cardiomyocytes ($p < 0.05$) (left).

Furthermore, here, we also examined the effect of Tica treatment of MetS rats on the protein expression level of SERCA2 in the cardiomyocyte homogenates. SERCA2 levels in those three groups were similar (Fig. 5E). However, since SERCA2 activity is regulated by phospholamban (PLB, though its phosphorylation level), we examined the phosphorylated PLB (pPLB) level together with PLB protein level in the treated and untreated MetS groups. The pPLB level in the MetS group was significantly depressed ($p < 0.05$), while Tica treatment-induced a very marked increase in the phosphorylation of PLB ($p < 0.05$) with no effect on its total protein level (Fig. 5F, left and right, respectively). The ratio of SERCA2 to pPLB was low in the MetS group compared to that of the control. That ratio was found to be significantly augmented in the treated MetS group (data not presented).

Effect of ticagrelor treatment on the function and ultrastructure of mitochondria of left ventricular cardiomyocytes from the MetS rats

In these group examinations, we first determined the mitochondrial membrane potential ($\Delta\Psi$m) in left ventricular cardiomyocytes. As can be seen in Fig. 6A, $\Delta\Psi$m was significantly depolarized in the MetS group in comparison to that of the control group. However, the Tica treatment of MetS rats for 2 weeks, fully preserved those changes. The original representative cells to $\Delta\Psi$m recordings are given in the left of Fig. 6A.

Second, we examined the ultrastructure of isolated cardiomyocytes using transmission electron microscopy, particularly focusing on the mitochondrial morphology and then quantitative analysis of those micrographs. The representative images are given in Fig. 6B. The images for the control group cardiomyocytes are given on the left of the images. Besides, there were irregularly partitioned and clustered mitochondria, increased numbers of lysosomes, enlarged SR, and T tubules system in the cardiomyocytes of the MetS rats (middle). There are also markedly suppressed mitochondrial fragmentation as well as well-organized Z lines and

T-tubular system including SR in the ultrastructural appearance of cardiomyocytes from the Tica-treated group. Furthermore, we determined markedly increased numbers of accumulated autophagosomes in the cytoplasm and autolysosomes containing residue bodies in some areas in the cardiomyocytes from MetS rats. Besides, mitochondrial disarray was also noted above and below of each sarcomere with a high degree of clustered irregular shaped mitochondria (a significant amount of round shape mitochondrion) in the MetS cardiomyocytes. Notably, Tica treatment could preserve not fully but partially the alterations which imply a recovery in mitochondrial fragmentation. However, to quantify the organization and morphology of the interfibrillar subpopulation of mitochondria, we calculated the percentage of mitochondria in each sarcomere length. As can be seen in Fig. 6C, the percentage of mitochondria in one sarcomere length increased by threefold in the MetS cardiomyocytes. Also, the percentages of mitochondria both equal to one sarcomere length and greater than one sarcomere length (elongated mitochondria) in the MetS group were significantly low compared to those of controls. The Tica treatment could preserve not fully but significantly those changes.

Since mitochondria constantly undergo fusion and fission processes, to support the beneficial effect of Tica on the MetS-associated changes in mitochondrial function, we also examined protein levels related to those processes in mitochondria such as Mfn-1 and Mfn-2 in the isolated cardiomyocytes. As can be seen in Fig. 6 (D and E), the Mfn-1 protein level was significantly high ($p < 0.05$), while the Mfn-2 was low in the MetS group ($p < 0.05$), whereas the Tica treatment was sufficient to restore the alteration in the Mfn-1 but not in the Mfn-2.

The ticagrelor treatment of MetS rats can preserve the SR function through augmentation in the ER stress markers

We examined the protein levels of two ER stress markers, calregulin, and GRP78. As can be seen in Fig. 7 (B and C, respectively), the protein expression levels of both markers were increased significantly in the MetS rat heart compared to that of control ($p < 0.05$). The Tica treatment of the MetS rats reversed those stress parameters, significantly ($p < 0.05$). The representative original Western protein bands of these proteins are given in Fig. 7A.

The ticagrelor treatment reversed the miscommunication between SR and mitochondria developed in the cardiomyocytes from the MetS rat heart

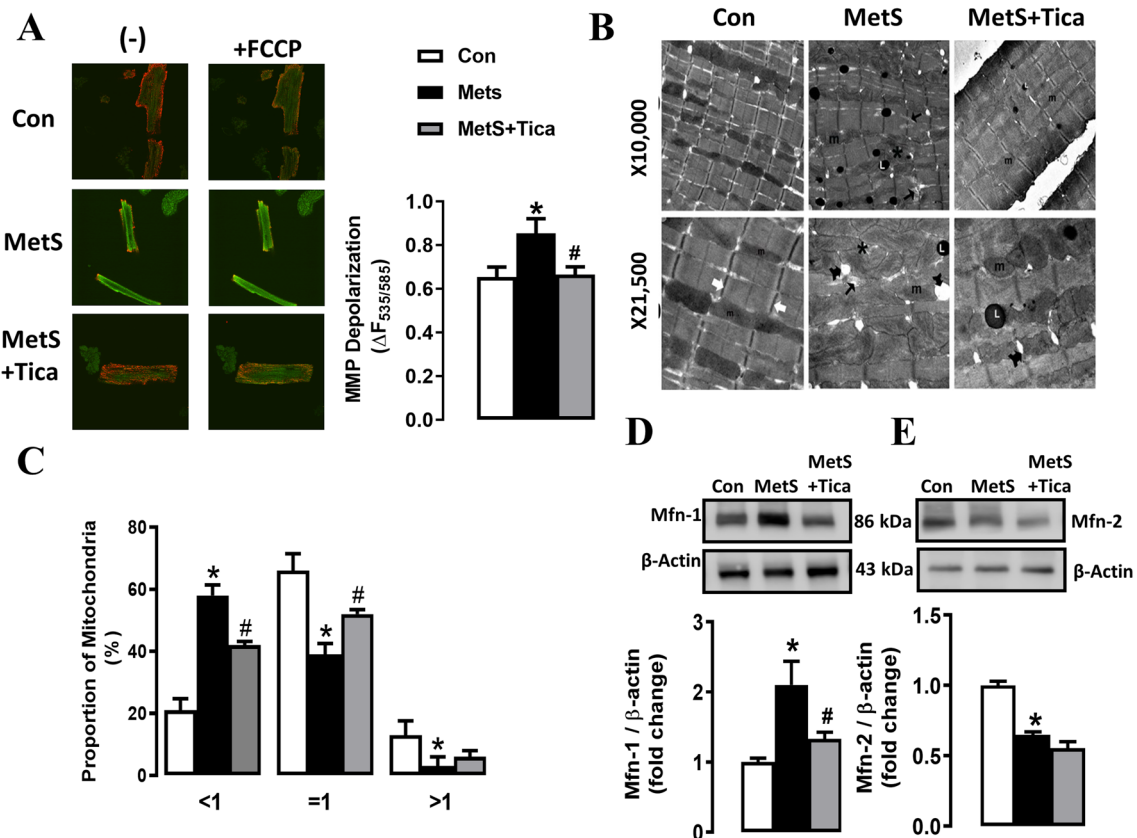Here, we examined the protein expression level of promyelocytic leukemia protein (PML), which plays an important

Fig. 6 Ticagrelor treatment of MetS rats markedly preserved the function and ultrastructure of mitochondria. (**A**) The representative images to determine the mitochondrial membrane potential (ΔΨm), as fluorescence intensity changes, in JC-1 loaded cardiomyocytes (5-μM for 30 min at 37 °C) (left) and their average values in experimental groups (right). (**B**) Transmission electron microscopy analysis of cardiomyocytes from Tica-treated Mets rat heart comparison to those of untreated MetS cardiomyocytes. Representative electron micrographs of isolated cardiomyocytes from both groups, irregularly partitioned and clustered mitochondria, numerous lysosomes, enlargement SR and T tubules (middle) with normal appearance in the control group (left). Regular mitochondrial arrangement and slightly decreased mitochondrial fragmentation, normal appearance of Z lines, SR, and T tubules in the Tica-treated MetS group (right). (**C**) The quantification of the images is presented as the organization and morphology of the interfibrillar subpopulation of mitochondria presented as the percentage of mitochondria in each sarcomere length. Shorten symbols: *m* mitochondrion, *L* lysosome, *arrow* sarcoplasmic reticulum cisternae, *tailed arrow* T tubules, *Asterix* partitioned mitochondria. The protein expression levels of mitochondrial proteins such as Mfn-1 (**D**) and Mfn-2 (**E**). The representative Western-blot bands are given in the upper part of the bars. The bars are representing the changes as mean (± SEM). The cells used are from the hearts of 4–5 rats/group. *$p < 0.05$ *vs.* Con group and #$p < 0.05$ *vs.* MetS group

role in proper communication between SR and mitochondria. As can be seen in Fig. 7D, the protein expression level of PML was significantly depressed in the Mets rat heart compared to that of the control ($p < 0.05$). The Tica treatment of Mets rats significantly reversed the depressed level of PML ($p < 0.05$).

We also examined another intracellular factor, which is responsible for a proper mitochondria function, casein kinase-2α (CK2α). We first determined the phosphorylation and protein expression levels of CK2α in the isolated cardiomyocytes from the MetS rat heart. In comparison to those of controls, its phosphorylation level (but not protein level) was about twofold higher in the MetS group. Besides, that phosphorylation was fully normalized with the Tica

treatment (Fig. 7F and G, respectively). The representative protein bands of these proteins are given in Fig. 7E.

The ticagrelor treatment reversed the increased oxidative stress in the MetS rat heart at both cellular and tissue levels

In another group experiment, we determined the intracellular ROS level in the isolated cardiomyocytes loaded with a cellular ROS-sensitive fluorescent dye, DCFDA (5-μM for 1-h incubation). By measuring confocal intensity changes in these DCFDA loaded cells, we determined the differences between these two groups as responses to H_2O_2 exposure (as % changes). The responses in the MetS rat cells were
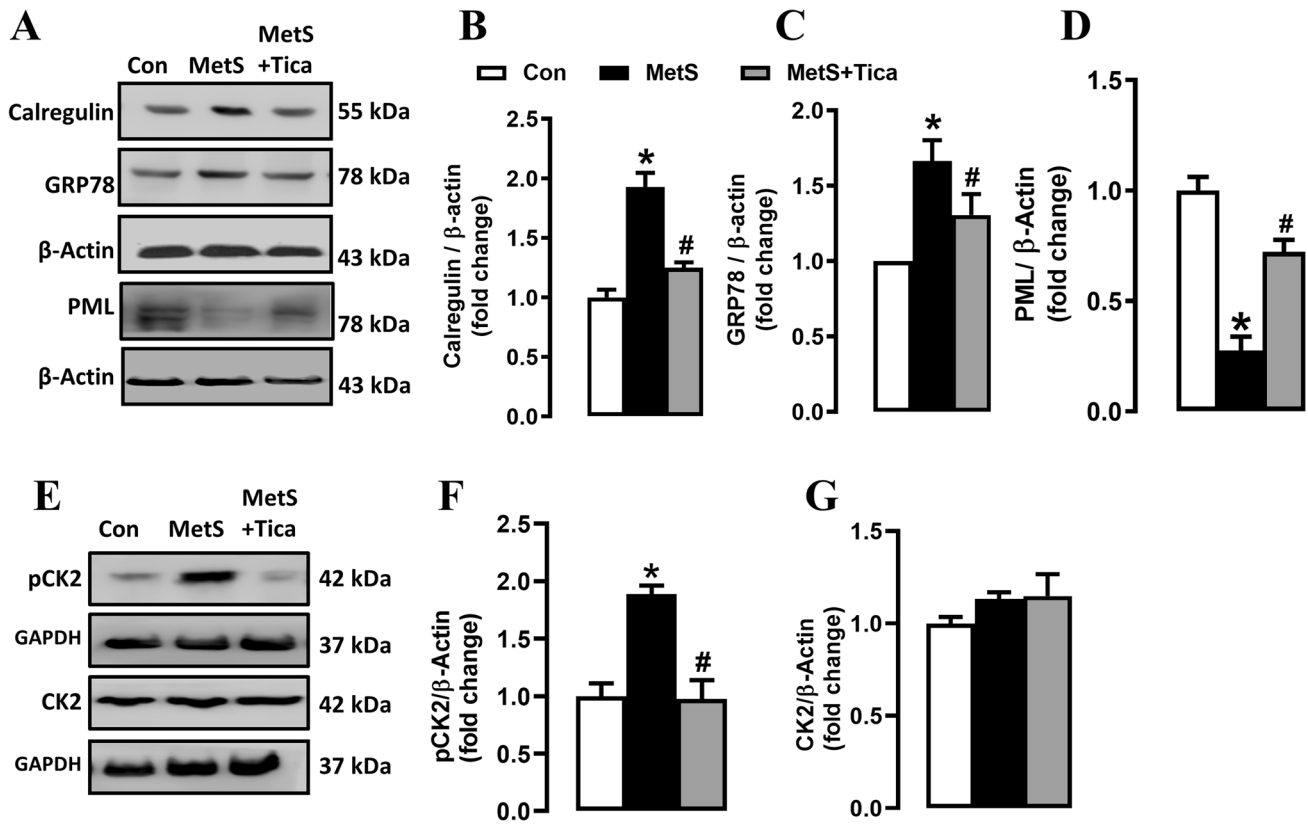
Fig. 7 Ticagrelor treatment of MetS rats preserved the ER stress markers and miscommunication between SR and mitochondria. (**A**) Representative Western-blot protein bands for calregulin, GRP78, and PML comparison to that of β-actin. The protein expression levels of calregulin (**B**), GRP78 (**C**), and PML (**D**). Representative Western-blot analysis of phosphorylation and protein levels of casein kinase 2α (CK2α) (**E**). The mean (± SEM) values of CK2α (**F**) and its protein expression levels (**G**). All bars are representing the changes as mean (± SEM). The number of hearts is 4–5, and the number of cells is 15–20 for each measurement. *$p < 0.05$ *vs.* Con group and #$p < 0.05$ *vs.* MetS group

significantly less than those of control rat cells ($p < 0.05$), indicating high ROS production in those cardiomyocytes. Therefore, the average ROS level in the MetS rat cardiomyocytes was significantly high in comparison to that of the control ($p < 0.05$) (Fig. 8B). Furthermore, to examine the role of Tica treatment on mitochondria-associated ROS production, we also measured the ROS production in the Tica-treated MetS group. As can be seen in that figure, the ROS level was fully rescued to the level of control. The original representative cells to ROS recordings are given in the left of Fig. 8A.

Similar to our previous study [5], TOS level (Fig. 8C) in the heart from the MetS rats was significantly high compared to those of the controls ($p < 0.05$), while TAS (Fig. 8D) was significantly low compared with those of controls ($p < 0.05$). Interestingly, although any direct antioxidant action of Tica has not been shown yet, Tica treatment of MetS rats elicited positive effects in the oxidative stress status of the heart tissue in the MetS rats.

Here, we also examined an endothelial enzyme NO synthase (NOS3), which generates nitric oxide (NO) and

catalyzes the conversion of L-arginine to L-citrulline. Phosphorylated NOS3 level was twofold higher in the cardiomyocytes from the MetS rats compared to those of controls, while the Tica treatment was able to normalize it, fully (Fig. 8F, left). However, the protein levels of NOS3 were similar among these three groups (Fig. 8F, right). The representative Western-blot protein bands are given in Fig. 8E.

Discussion

In the present study, we evaluated the beneficial effects of Tica treatment in MetS rat heart function. This treatment did not provide significant improvement in high body weight and blood glucose level as well as insulin resistance. This treatment also no effect on in MetS rats. Importantly, our data presented that there is a significant amount of P2Y12 protein expression in isolated left ventricular cardiomyocytes from normal rats while that level was not changed in those of treated or untreated MetS cardiomyocytes, as well.
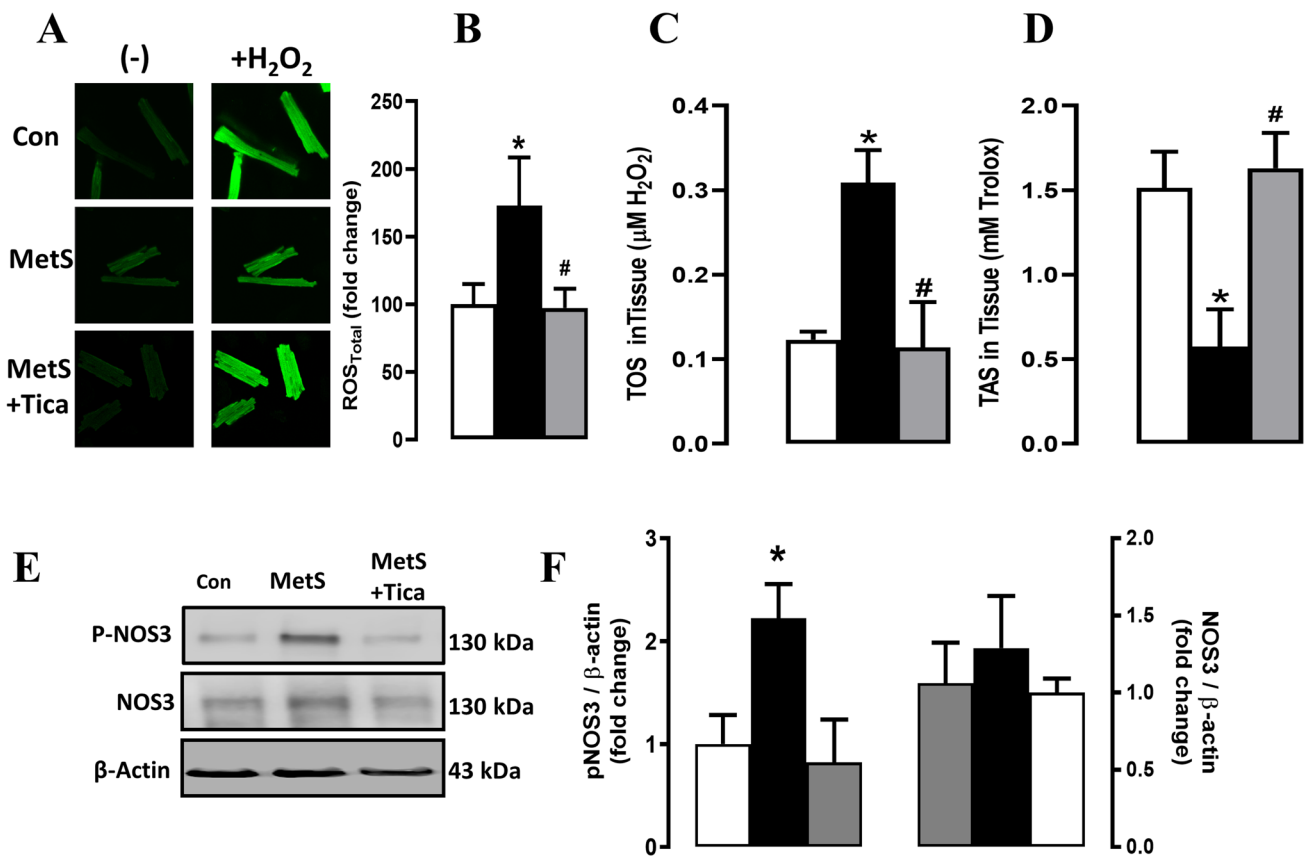
Fig. 8 Effects of the ticagrelor treatment on the increased oxidative stress in the MetS rat heart at both cellular and tissue levels. (**A**) The representative images to determine the increase of reactive oxygen species (ROS), as fluorescence intensity changes, in CM-H2DCFDA loaded (5-μM for 45 min at 37 °C) cardiomyocytes. (**B**) The average ROS values in experimental groups. (**C**) The total oxidative stress status (TOS) and the total antioxidant status (**D**) are measured in the heart tissue homogenates. (**E**) Representative Western-blot bands for phosphorylated and expression levels of endothelial NO synthase (NOS3). (**F**) The average (mean ± SEM) values for phospho-NOS3 (left) and protein expression level of NOS3 to β-actin (right). All bars are representing the changes as mean (± SEM). The number of hearts is 4–5, and the numbers of cells are 15–20 for each measurement. *$p < 0.05$ vs. Con group and #$p < 0.05$ vs. MetS group

Different pathological conditions (including hyperglycemia, insulin resistance, oxidative stress) can change the excitability of cardiomyocytes by influencing the individual type ion-channel activity [5, 32, 35, 36]. The present study demonstrated that the amplitude of APs was significantly high with significantly prolonged AP duration in freshly isolated left ventricular cardiomyocytes of the MetS rats compared to those of age-matched controls. Our further examinations demonstrated that the higher amplitude of APs is closely associated with enhanced Na$^+$-influx due to increased voltage-dependent I_{Na} while the slower depolarization rate in APs is associated, at most, with slower inactivation of I_{Na}. This observation was also can be associated with other factors responsible for Na$^+$-influx such as Na$^+$/glucose co-transporter activation. Furthermore, the examinations of both the I_{CaL} and I_K have also shown that I_K was significantly depressed in the MetS group with no change in I_{CaL} contributing to prolongation in the repolarization phases of APs in those cells. Of

note, a slight but significant increase in the I_{NCXout} may mediate the prolonged APs duration in the MetS group. More importantly, those above parameters of APs and the ionic mechanisms contributing to the configuration of APs in the treated group were significantly reversed. A supporting study has been recently published by Cheng et al., who demonstrated the cardioprotective effect of Tica pretreatment of the animals following myocardial infarction (MI) through the recoveries in the electrophysiological properties of stellate ganglion neurons, including improvement in the abnormalities of the I_{Na} and the I_K together with alterations in AP parameters [29]. Another study also demonstrated that Tica treatment, at clinically relevant concentration, has an inhibitory effect on the NCX1 in cardiac derived H9c2 cells, which can imply the possibility of cardiac NCX1 as a new downstream target of Tica and contribute to the therapeutic profile of Tica in clinical practice [37]. Overall, these groups of data suggest that Tica treatment exerts cardioprotective effects, potentially

through modulating the activity of different ion channels in the ventricular cardiomyocytes.

A proper excitation–contraction coupling in cardiomyocytes is closely associated with the intracellular free Ca^{2+} level, through strictly regulation of SR and mitochondria [38–40]. It is known that I_{CaL} and the I_{NCXout} mediate Ca^{2+} entry in ventricular cardiomyocytes. Here, the I_{CaL} was not changed with MetS, however we cannot exclude the contribution of slightly increased I_{NCXout} to increase in the resting intracellular Ca^{2+} level in the MetS group. More importantly, as described previously [41], here, we determined significantly increased $\Delta F/F_0$ level in the cardiomyocytes from the MetS group, suggesting the increases in the diastolic Ca^{2+} level, which in turns, leads to depression in the contractile activity of the heart [5, 41]. The main underlying factor to increase in Ca^{2+} level seems to be associated with the depressed function of SR, as well. In the present study, similar to our previous studies [5, 41], we also have shown that there was a leaky-SR, at most, due to the hyperphosphorylation of RyR2 and dephosphorylation of PLB in the cardiomyocytes from the MetS rats. Tica treatment of the MetS rats significantly prevented those changes and provided a proper SR function. Further analysis of those cardiomyocytes from Tica-treated MetS rats with electron microscopy demonstrated marked recoveries in the ultrastructure of cardiomyocytes such as restoration in the enlargement of SR and T tubules, which are also supporting the recovery in SR function. Furthermore, our present data demonstrated that there is significant improvement in the activated ER stress markers with Tica treatment of the MetS rats. Furthermore, these findings are in line with our previously published data. In that in vitro cell-line study, we have shown that Tica treatment of insulin-resistant H9c2-myocytes reversed the markedly activated ER stress markers, as well [6]. There are several data in the literature supporting our present data. Correspondingly, other studies demonstrated an important protective effect of Tica against endothelial dysfunction through diminution of ER stress and attenuation of ROS increase, at most, through its off-target activity other than antagonistic action [42].

The Tica treatment of the MetS rats provided significant augmentation in the function and ultrastructure of mitochondria, which were previously demonstrated in a similar group of MetS rat studies [5, 34]. Particularly, Tica treatment reversed the depolarized $\Delta\Psi m$, which are supported with recoveries in mitochondrial ultrastructure such as marked recovery in the increased number of mitochondrial fragmentations. Indeed, recently, our in vitro cell-line study has also shown that Tica reverses mitochondrial dysfunction by preventing the increased numbers of accumulated autophagosomes as well as autophagosomes-dependent apoptosis in insulin-resistant H9c2-myocytes [6]. The reversed protein level of Mnf-1 but not Mfn-2 (it is also an indicator of

insulin resistance) determined in the cardiomyocytes from the Tica-treated MetS group also can imply a partial recovery in the cardiomyocytes under the present experimental condition.

Previously, authors demonstrated the presence of CK2 in purified mitochondria and it appears that the effect on $\Delta\psi m$ and mitochondrial permeability through its important regulatory role in intracellular Ca^{2+}-signaling [43, 44]. Furthermore, the important regulatory roles of cytosolic kinases (including CK2) on mitochondrial protein import has been also demonstrated [45]. Thus, our data showing the high phosphorylation level of CK2α can also imply the beneficial effect of Tica treatment on the preservation of mitochondrial function in the MetS rat cardiomyocytes.

Since autophagy plays a key role in the maintenance of cellular homeostasis, suppressing Ca^{2+} transfer between SR and mitochondria under increased oxidative stress [22, 46]. Furthermore, our data on reversed protein level of PML with Tica treatment pointed out the recovery between SR and mitochondria cross-talk, most probably affecting the control of autophagy [24, 25]. More importantly, our present data, once more, emphasize the current awareness about the central role of mitochondrial abnormalities in the development of cardiac dysfunction in insulin-resistant heart, especially in the MetS condition [47].

Taken into consideration the relation between increased oxidative stress and mitochondria dysfunction and further their roles in cardiovascular disorders (particularly alterations in SR–mitochondria axis) together with already known actions of Tica [30], we determined the oxidative stress status in the isolated cardiomyocytes as well as in the heart tissue level. Confocal imaging of not only ROS production level in the cells but also the phosphorylation level of NOS3 was found to be significantly high in the MetS group while they were fully reversed in the Tica-treated group. Moreover, the increased level of TOS in the heart tissue was fully normalized with a fully normal TAS level in the Tica-treated MetS group. A supporting study presented that Tica treatment of high-fat diet-induced hypercholesterolemic mice provided important benefits on atherosclerosis through inducing increases in paraoxonase-1 [48].

Likewise, Tica treatment restored the apoptosis rate, in a dose-dependent manner, as well as significantly increased the expression levels of Akt, p-Akt, Bcl-2, eNOS, and NO concentration, and significantly decreased the expression levels of Bax and caspase-3. Therefore, similar to our suggestion, they explained their Tica-associated benefits by Tica-induced recoveries in apoptosis and antioxidant pathways [49]. As documented in many articles, mitochondrial abnormalities have been reported in both insulin-deficient and insulin-resistant states [50, 51], and overproduction of mitochondrial ROS leads not only to mitochondrial but also to cellular oxidative damage in diabetes [52]. The existence

of adverse risk factors for the occurrence of cardiac dysfunction in MetS is still unclear, therefore, unraveling the mechanisms involved in the onset of MetS-associated heart dysfunction will improve the understanding of its pathophysiology, and will provide new horizons for novel therapeutic targets in MetS patients. Interestingly, recent meta-analysis studies demonstrated that Tica treatment of patients with type 2 diabetes mellitus besides other cardiac dysfunctions provided a cardioprotective effect through affecting the oxidative stress biomarkers such as MDA and GSH [19, 53–55]. Wang et al. [42] demonstrated that treatment of male rats with Tica for 14-day protected against AngII-induced endothelial dysfunction via preventing increased ROS production, eNOS phosphorylation, and ameliorating the ER stress.

Interestingly, Mokhtar et al. presented a wide review of the data with clinical interventions and they discussed the pleiotropic effects of Tica whether myth or reality [56]. In their discussion, they analyzed the clinical benefit of Tica in patients with an acute coronary syndrome and suggested that the benefit was due to its off-target property [18]. Later observations have led to a hypothesis that Tica has pleiotropic properties, providing some novel benefits, via the non-platelet-directed mechanism of action in different types of pathological conditions, including diabetes [17, 18, 57, 58].

The contact state between mitochondria and SR is critical in various processes, such as ER stress, apoptosis, autophagy, and Ca^{2+} handling [22, 46]. New functions of their contact sites in hormonal and nutrient signaling recently emerged, thus highlighting the dynamic regulation of SR–mitochondria interactions in function of energy state and nutrient status [23]. In agreement with several studies, mitochondrial dysfunction and ER stress have been largely and independently associated with metabolic diseases, such as obesity or type 2 diabetes mellitus [59, 60]. Furthermore, metabolic homeostasis in mammalians is dependent on proper signaling pathways from SR, such as the unfolded protein response and the autophagy, both controlled by mitochondrial membranes integrity and by mitochondria-associated membranes (MAM) actors, which are an important hub for several signaling pathways controlling metabolic homeostasis as well as insulin signaling [61]. Considering those studies together with our present data strongly imply the important role of Tica on miscommunication between SR and MAM in the insulin-resistant MetS rat cardiomyocytes. Furthermore, supporting our interpretation, recent studies highlight that SR–mitochondria miscommunication in different tissues could contribute to metabolic diseases [30, 61]. In most of those studies, it has been pointed out the importance of looking for regulatory players of the SR–mitochondria cross-talk to treat metabolic diseases. More interestingly, in a recent study performed under in vitro condition, researchers demonstrated that Tica enhances release of anti-hypoxic cardiac progenitor cell-derived exosomes, which further support the development of novel clinically relevant pharmacological interventions for Tica for exosome-based cardioprotection, through activation of the equilibrative nucleoside transporter 1 [62]. That finding also may enhance the clinical significance of Tica usage in the development of new noninvasive pharmacological approach to protect heart at risk for developing myocardial ischemic injury. However, these observations are still in the initial stages to determine whether SR–mitochondria miscommunication contributes to metabolic diseases.

Overall, taken into consideration the existence of P2Y12 receptors in left ventricular cardiomyocytes, one can suggest that the effect and clinical benefit of Tica cannot be limited to platelet inhibition in patients with cardiovascular disorders. Indeed, Tica is also unique in having the only well-documented additional target of inhibition, such as the equilibrative nucleoside transporter 1, which has a role in the prevention of accumulated autophagosomes-dependent apoptosis and ER stress in insulin-resistant H9c2-myocytes as well [6]. As summarized in Fig. 9, there is a marked development of cardiometabolic syndrome in high-carbohydrate intake induced MetS mammalians, which induces an important level of increased oxidative/nitrosative stress in the cardiomyocytes. Those also lead to dysfunctions in the sarcolemma, SR, and mitochondria, which in turn further leads to cardiomyocyte dysfunction. Tica treatment can affect the miscommunication between SR–mitochondria sites, thereby provides important benefits for cardiac dysfunction in MetS individuals. In summary, our study reveals a novel pharmacological function of Tica in addition to its classic antiplatelet properties, which suggests that it may serve as a potential therapeutic agent for use in MetS-associated heart diseases.
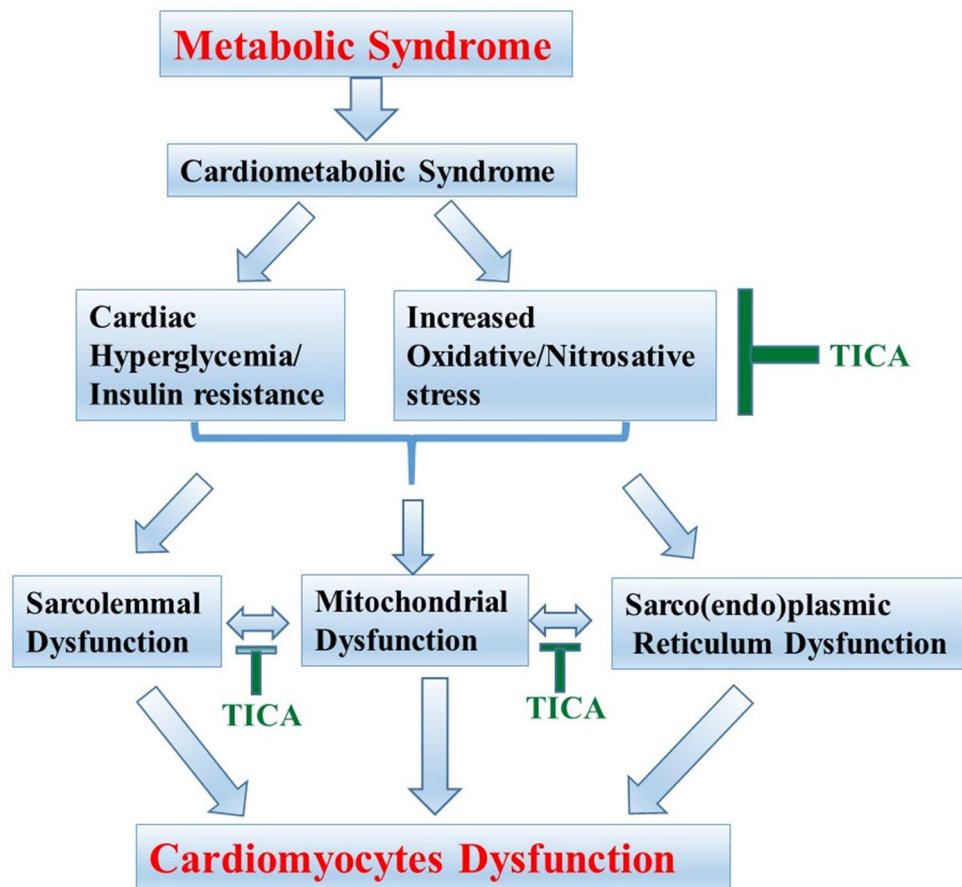
Fig. 9 A possible pathway underlying the pleiotropic effects of ticagrelor in electrical activity of ventricular cardiomyocytes from high-carbohydrate intake induced metabolic syndrome rats through affecting sarcoplasmic reticulum-mitochondria miscommunication. High-carbohydrate intake can induce cardiometabolic syndrome in mammalians with metabolic syndrome, which is closely associated with hyperglycemia and insulin resistance as well as development of increased oxidative and nitrosative stress at both cellular and tissue levels besides systemic level. Both pathophysiological states are also closely related with alterations in organelle level such as alterations in either sarcoplasmic reticulum, mitochondria, or both as well as miscommunication between organelles such as sarcoplasmic reticulum-mitochondria cross-talk. Ticagrelor (TICA) treatment of metabolic syndrome rats may induce pleiotropic effects on oxidative/nitrosative stress and therefore can preserve the miscommunication between sarcoplasmic reticulum and mitochondria, behind its antiplatelet action

Author contributions B.T. designed and supervised the research and provided the final approval of the version to be published; S.O. supervised the research and contributed to the editing of the manuscript; Y.O., E.T., A.D, and S.D. contributed and performed the experiments and analyzed the data; D.B. performed all light and electron microscopic analysis. All authors discussed the results and commented on the manuscript.

Data availability The data used to support the findings of this study are available from the corresponding author upon reasonable request.

Declarations

Conflict of interest The authors declare no conflicts of interest.

Informed consent All experimental protocols were approved by the Institutional Animal Care and Use Committee of the Ankara University. All animals received human care under an institutionally approved experimental animal protocol with ethical license in Turkey.

References

1. Kahn R (2005) Buse J Ferrannini E y cols. The metabolic syndrome: time for a critical appraisal: joint statement from the American Diabetes Association and European Association for the Study of Diabetes. Diabetes Care 28:2289–2304
2. Cornier M-A, Dabelea D, Hernandez TL, Lindstrom RC, Steig AJ, Stob NR, Van Pelt RE, Wang H, Eckel RH (2008) The metabolic syndrome. Endocr Rev 29:777–822
3. Abel ED, Litwin SE, Sweeney G (2008) Cardiac remodeling in obesity. Physiol Rev 88:389–419

4. Durak A, Olgar Y, Tuncay E, Karaomerlioglu I, Kayki Mutlu G, Arioglu Inan E, Altan VM, Turan B (2017) Onset of decreased heart work is correlated with increased heart rate and shortened QT interval in high-carbohydrate fed overweight rats. Can J Physiol Pharmacol 95:1335–1342

5. Durak A, Olgar Y, Degirmenci S, Akkus E, Tuncay E, Turan B (2018) A SGLT2 inhibitor dapagliflozin suppresses prolonged ventricular-repolarization through augmentation of mitochondrial function in insulin-resistant metabolic syndrome rats. Cardiovasc Diabetol 17:1–17

6. Olgar Y, Tuncay E, Billur D, Durak A, Ozdemir S, Turan B (2020) Ticagrelor reverses the mitochondrial dysfunction through preventing accumulated autophagosomes-dependent apoptosis and ER stress in insulin-resistant H9c2 myocytes. Molecular and Cellular Biochemistry. https://doi.org/10.1007/s11010-020-03731-9

7. Hollopeter G, Jantzen H-M, Vincent D, Li G, England L, Ramakrishnan V, Yang R-B, Nurden P, Nurden A, Julius D (2001) Identification of the platelet ADP receptor targeted by antithrombotic drugs. Nature 409:202–207

8. Simon J, Filippov AK, Göransson S, Wong YH, Frelin C, Michel AD, Brown DA, Barnard EA (2002) Characterization and channel coupling of the P2Y(12) nucleotide receptor of brain capillary endothelial cells. J Biol Chem 277:31390–31400. https://doi.org/10.1074/jbc.M110714200

9. Wihlborg A-K, Wang L, Braun OO, Eyjolfsson A, Gustafsson R, Gudbjartsson T, Erlinge D (2004) ADP receptor P2Y12 is expressed in vascular smooth muscle cells and stimulates contraction in human blood vessels. Arterioscler Thromb Vasc Biol 24:1810–1815

10. Kawaguchi A, Sato M, Kimura M, Ichinohe T, Tazaki M, Shibukawa Y (2015) Expression and function of purinergic P2Y12 receptors in rat trigeminal ganglion neurons. Neurosci Res 98:17–27. https://doi.org/10.1016/j.neures.2015.04.008

11. Sasaki Y, Hoshi M, Akazawa C, Nakamura Y, Tsuzuki H, Inoue K, Kohsaka S (2003) Selective expression of Gi/o-coupled ATP receptor P2Y12 in microglia in rat brain. Glia 44:242–250. https://doi.org/10.1002/glia.10293

12. Gachet C (2012) P2Y(12) receptors in platelets and other hematopoietic and non-hematopoietic cells. Purinergic Signal 8:609–619. https://doi.org/10.1007/s11302-012-9303-x

13. Yang H, Tang B, Xu CH, Ahmed A (2019) Ticagrelor versus prasugrel for the treatment of patients with Type 2 diabetes mellitus following percutaneous coronary intervention: a systematic review and meta-analysis. Diabetes Therapy 10:81–93

14. Åkerblom A, Wojdyla DM, Wallentin L, James SK, de Souza BF, Steg PG, Cannon CP, Katus HA, Himmelmann A, Storey RF (2019) Ticagrelor in patients with heart failure after acute coronary syndromes—Insights from the PLATelet inhibition and patient Outcomes (PLATO) trial. Am Heart J 213:57–65

15. Sweeny JM, Angiolillo DJ, Franchi F, Rollini F, Waksman R, Raveendran G, Dangas G, Khan ND, Carlson GF, Zhao Y (2017) Impact of diabetes mellitus on the pharmacodynamic effects of ticagrelor versus clopidogrel in troponin-negative acute coronary syndrome patients undergoing ad hoc percutaneous coronary intervention. Journal of the American Heart Association 6:e005650

16. Franchi F, Rollini F, Aggarwal N, Hu J, Kureti M, Durairaj A, Duarte VE, Cho JR, Been L, Zenni MM (2016) Pharmacodynamic comparison of prasugrel versus ticagrelor in patients with type 2 diabetes mellitus and coronary artery disease: the OPTIMUS (Optimizing Antiplatelet Therapy in Diabetes Mellitus)-4 study. Circulation 134:780–792

17. Mansour A, Bachelot-Loza C, Nesseler N, Gaussem P, Gouin-Thibault I (2020) P2Y12 Inhibition beyond Thrombosis: Effects on Inflammation. Int J Mol Sci 21:1391

18. Nylander S, Schulz R (2016) Effects of P2Y12 receptor antagonists beyond platelet inhibition–comparison of ticagrelor with thienopyridines. Br J Pharmacol 173:1163–1178

19. Schnorbus B, Daiber A, Jurk K, Warnke S, König J, Krahn U, Lackner K, Munzel T, Gori T (2014) Effects of clopidogrel, prasugrel and ticagrelor on endothelial function, inflammatory and oxidative stress parameters and platelet function in patients undergoing coronary artery stenting for an acute coronary syndrome. A randomised, prospective, controlled study. BMJ open. https://doi.org/10.1136/bmjopen-2014-005268

20. Serebruany VL, Atar D (2010) The PLATO trial: do you believe in magic? Oxford University Press

21. Audia JP, Yang X-M, Crockett ES, Housley N, Haq EU, O'Donnell K, Cohen MV, Downey JM, Alvarez DF (2018) Caspase-1 inhibition by VX-765 administered at reperfusion in P2Y 12 receptor antagonist-treated rats provides long-term reduction in myocardial infarct size and preservation of ventricular function. Basic Res Cardiol 113:32

22. Tubbs E, Rieusset J (2017) Metabolic signaling functions of ER–mitochondria contact sites: role in metabolic diseases. J Mol Endocrinol 58:R87–R106

23. López-Crisosto C, Bravo-Sagua R, Rodriguez-Peña M, Mera C, Castro PF, Quest AF, Rothermel BA, Cifuentes M, Lavandero S (2015) ER-to-mitochondria miscommunication and metabolic diseases. Biochimica et Biophysica Acta (BBA)-Molecular Basis of Disease 1852:2096–2105

24. Missiroli S, Danese A, Iannitti T, Patergnani S, Perrone M, Previati M, Giorgi C, Pinton P (2017) Endoplasmic reticulum-mitochondria Ca2+ crosstalk in the control of the tumor cell fate. Biochimica et Biophysica Acta (BBA)-Molecular Cell Research 1864:858–864

25. Pinton P, Giorgi C, Pandolfi P (2011) The role of PML in the control of apoptotic cell fate: a new key player at ER–mitochondria sites. Cell Death Differ 18:1450–1456

26. Gale EA (2005) The myth of the metabolic syndrome. Springer

27. Huang B, Qian Y, Xie S, Ye X, Chen H, Chen Z, Zhang L, Xu J, Hu H, Ma S (2020) Ticagrelor inhibits the NLRP3 inflammasome to protect against inflammatory disease independent of the P2Y 12 signaling pathway. Cellular & Molecular Immunology 18:1278–1289

28. Penna C, Aragno M, Cento AS, Femminò S, Russo I, Bello FD, Chiazza F, Collotta D, Alves GF, Bertinaria M (2020) Ticagrelor Conditioning Effects Are Not Additive to Cardioprotection Induced by Direct NLRP3 Inflammasome Inhibition: Role of RISK, NLRP3, and Redox Cascades. Oxidative Medicine and Cellular Longevity. https://doi.org/10.1155/2020/9219825

29. Cheng L, Fu H, Wang X, Ye L, Lakhani I, Tse G, Zhang Z, Liu T, Li G (2020) Effects of ticagrelor pretreatment on electrophysiological properties of stellate ganglion neurons following myocardial infarction. Clin Exp Pharmacol Physiol 47:1932–1942

30. Sebastián D, Hernández-Alvarez MI, Segalés J, Sorianello E, Muñoz JP, Sala D, Waget A, Liesa M, Paz JC, Gopalacharyulu P (2012) Mitofusin 2 (Mfn2) links mitochondrial and endoplasmic reticulum function with insulin signaling and is essential for normal glucose homeostasis. Proc Natl Acad Sci 109:5523–5528

31. Erel O (2004) A novel automated direct measurement method for total antioxidant capacity using a new generation, more stable ABTS radical cation. Clin Biochem 37:277–285. https://doi.org/10.1016/j.clinbiochem.2003.11.015

32. Turan B, Desilets M, Acan LN, Hotomaroglu O, Vannier C, Vassort G (1996) Oxidative effects of selenite on rat ventricular contractility and Ca movements. Cardiovasc Res 32:351–361

33. Tuncay E, Olgar Y, Durak A, Degirmenci S, Bitirim CV, Turan B (2019) β3-adrenergic receptor activation plays an important role in the depressed myocardial contractility via both elevated levels

of cellular free Zn2+ and reactive nitrogen species. J Cell Physiol 234:13370–13386

34. Durak A, Bitirim CV, Turan B (2020) Titin and CK2α are New Intracellular Targets in Acute Insulin Application-Associated Benefits on Electrophysiological Parameters of Left Ventricular Cardiomyocytes From Insulin-Resistant Metabolic Syndrome Rats. Cardiovascular drugs and therapy. https://doi.org/10.1007/s10557-020-06974-2

35. Ozdemir S, Ugur M, Gürdal H, Turan B (2005) Treatment with AT1 receptor blocker restores diabetes-induced alterations in intracellular Ca2+ transients and contractile function of rat myocardium. Arch Biochem Biophys 435:166–174

36. Bilginoglu A, Kandilci HB, Turan B (2013) Intracellular levels of Na+ and TTX-sensitive Na+ channel current in diabetic rat ventricular cardiomyocytes. Cardiovasc Toxicol 13:138–147

37. Lariccia V, Macrì ML, Matteucci A, Maiolino M, Amoroso S, Magi S (2019) Effects of ticagrelor on the sodium/calcium exchanger 1 (NCX1) in cardiac derived H9c2 cells. Eur J Pharmacol 850:158–166

38. Rossini M, Filadi R (2020) Sarcoplasmic Reticulum-Mitochondria Kissing in Cardiomyocytes: Ca2+, ATP, and Undisclosed Secrets. Frontiers in Cell and Developmental Biology 8:532

39. Eisner DA, Caldwell JL, Kistamás K, Trafford AW (2017) Calcium and excitation-contraction coupling in the heart. Circ Res 121:181–195

40. Andrienko TN, Picht E, Bers DM (2009) Mitochondrial free calcium regulation during sarcoplasmic reticulum calcium release in rat cardiac myocytes. J Mol Cell Cardiol 46:1027–1036

41. Okatan EN, Durak AT, Turan B (2016) Electrophysiological basis of metabolic-syndrome-induced cardiac dysfunction. Can J Physiol Pharmacol 94:1064–1073

42. Wang X, Han X, Li M, Han Y, Zhang Y, Zhao S, Li Y (2018) Ticagrelor protects against AngII-induced endothelial dysfunction by alleviating endoplasmic reticulum stress. Microvasc Res 119:98–104. https://doi.org/10.1016/j.mvr.2018.05.006

43. Afzal M, Kren BT, Naveed AK, Trembley JH, Ahmed K (2020) Protein kinase CK2 impact on intracellular calcium homeostasis in prostate cancer. Molecular and Cellular Biochemistry. https://doi.org/10.1007/s11010-020-03752-4

44. Qaiser F, Trembley JH, Kren BT, Wu JJ, Naveed AK, Ahmed K (2014) Protein kinase CK2 inhibition induces cell death via early impact on mitochondrial function. J Cell Biochem 115:2103–2115

45. Schmidt O, Harbauer AB, Rao S, Eyrich B, Zahedi RP, Stojanovski D, Schönfisch B, Guiard B, Sickmann A, Pfanner N (2011) Regulation of mitochondrial protein import by cytosolic kinases. Cell 144:227–239

46. Szymański J, Janikiewicz J, Michalska B, Patalas-Krawczyk P, Perrone M, Ziółkowski W, Duszyński J, Pinton P, Dobrzyń A, Więckowski MR (2017) Interaction of mitochondria with the endoplasmic reticulum and plasma membrane in calcium homeostasis, lipid trafficking and mitochondrial structure. Int J Mol Sci 18:1576

47. Makrecka-Kuka M, Liepinsh E, Murray AJ, Lemieux H, Dambrova M, Tepp K, Puurand M, Kaambre T, Han WH, de Goede P, O'Brien KA, Turan B, Tuncay E, Olgar Y, Rolo AP, Palmeira CM, Boardman NT, Wust RCI, Larsen TS (2019) Altered mitochondrial metabolism in the insulin-resistant heart. Acta Physiol (Oxf). https://doi.org/10.1111/apha.13430

48. Halim H, Pinkaew D, Chunhacha P, Sinthujaroen P, Thiagarajan P, Fujise K (2019) Ticagrelor induces paraoxonase-1 (PON1) and better protects hypercholesterolemic mice against atherosclerosis compared to clopidogrel. PloS one 14:e0218934

49. Kang M, Shao S, Zhang Y, Liang X, Zhang K, Li G (2019) Beneficial Effects of Ticagrelor on Oxidized Low-Density Lipoprotein (ox-LDL)-Induced Apoptosis in Human Umbilical Vein Endothelial Cells. Med Sci Monit 25:9811

50. Fauconnier J, Lanner JT, Zhang SJ, Tavi P, Bruton JD, Katz A, Westerblad H (2005) Insulin and inositol 1,4,5-trisphosphate trigger abnormal cytosolic Ca2+ transients and reveal mitochondrial Ca2+ handling defects in cardiomyocytes of ob/ob mice. Diabetes 54:2375–2381. https://doi.org/10.2337/diabetes.54.8.2375

51. Yaras N, Ugur M, Ozdemir S, Gurdal H, Purali N, Lacampagne A, Vassort G, Turan B (2005) Effects of diabetes on ryanodine receptor Ca release channel (RyR2) and Ca2+ homeostasis in rat heart. Diabetes 54:3082–3088

52. Tuncay E, Turan B (2016) Intracellular Zn(2+) Increase in Cardiomyocytes Induces both Electrical and Mechanical Dysfunction in Heart via Endogenous Generation of Reactive Nitrogen Species. Biol Trace Elem Res 169:294–302. https://doi.org/10.1007/s12011-015-0423-3

53. Sharmin E, Dewan JF, Ahsan SA, Hoque H, Ahmed SF, Sultan MAU, Bhuiyan HA, Bhadra S, Barua C (2016) Effect of Ticagrerol versus Clopidogrel on Oxidative Stress Bio-markers in Patients with Chronic Stable Angina after Percutaneous Coronary Intervention. Univ Heart J 12:26–30

54. Navarese EP, Buffon A, Kozinski M, Obonska K, Rychter M, Kunadian V, Austin D, De Servi S, Sukiennik A, Kubica J (2013) A critical overview on ticagrelor in acute coronary syndromes. QJM 106:105–115

55. Tataruņas V, Kupstyte-Kristapone N, Zvikas V, Jakstas V, Zaliunas R, Lesauskaite V (2020) Factors associated with platelet reactivity during dual antiplatelet therapy in patients with diabetes after acute coronary syndrome. Sci Rep 10:3175. https://doi.org/10.1038/s41598-020-59663-3

56. Ait-Mokhtar O, Bonello L, Benamara S, Paganelli F (2012) High on Treatment Platelet Reactivity. Heart Lung Circ 21:12–21. https://doi.org/10.1016/j.hlc.2011.08.069

57. Bonello L, Laine M, Kipson N, Mancini J, Helal O, Fromonot J, Gariboldi V, Condo J, Thuny F, Frere C (2014) Ticagrelor increases adenosine plasma concentration in patients with an acute coronary syndrome. J Am Coll Cardiol 63:872–877

58. Jeong HS, Hong SJ, Cho S-A, Kim J-H, Cho JY, Lee SH, Joo HJ, Park JH, Yu CW, Lim D-S (2017) JACC 10:1646–1658

59. Chang Y-C, Hee S-W, Hsieh M-L, Jeng Y-M, Chuang L-M (2015) The role of organelle stresses in diabetes mellitus and obesity: implication for treatment. Analytical cellular pathology. https://doi.org/10.1155/2015/972891

60. Hasnain SZ, Prins JB, McGuckin MA (2016) Oxidative and endoplasmic reticulum stress in b-cell dysfunction in diabetes. J Mol Endocrinol 56:33–54

61. Tubbs E, Theurey P, Vial G, Bendridi N, Bravard A, Chauvin M-A, Ji-Cao J, Zoulim F, Bartosch B, Ovize M (2014) Mitochondria-associated endoplasmic reticulum membrane (MAM) integrity is required for insulin signaling and is implicated in hepatic insulin resistance. Diabetes 63:3279–3294

62. Valentina C, Matteucci M, Pasanisi EM, Papa A, Lucio B, Fritsche-Danielson R, Vincenzo L (2020) Ticagrelor Enhances Release of Anti-Hypoxic Cardiac Progenitor Cell-Derived Exosomes Through Increasing Cell Proliferation In Vitro. Scientific Reports (Nature Publisher Group). https://doi.org/10.1038/s41598-020-59225-7

Publisher's Note Springer Nature remains neutral with regard to jurisdictional claims in published maps and institutional affiliations.